Proc. NIPR Symp. Upper Atmos. Phys., **7**, 26–31, 1994

PLASMASPHERIC CAVITY-MODE MHD OSCILLATIONS WITH ENERGY FLOW ACROSS THE PLASMAPAUSE

Shigeru FUJITA[1] and Karl-Heinz GLASSMEIER[2]

[1]*Meteorological College, 7–81, Asahi 4-chome, Kashiwa 277*
[2]*Institut für Geophysik und Meteorologie, Technische Universität Braunschweig, 38106 Braunschweig, Federal Republic of Germany*

Abstract: Cavity-mode oscillations in the plasmasphere are studied under the assumption that the oscillation energy leaks across the outer boundary of the plasma-spheric cavity. This is a realistic assumption for the cavity-mode oscillations because the plasmapause cannot reflect perfectly the oscillation energy. Numerical calculations reveal that leakage significantly affects behavior of cavity-mode oscillations.

1. Introduction

Pi2 pulsations observed in mid- and low-latitudes are likely generated by impulsive energy injection into the plasmasphere (SUTCLIFFE and YUMOTO, 1989, 1991; YEOMAN and ORR, 1989; YUMOTO *et al.*, 1989; TAKAHASHI *et al.*, 1992).

The plasmaspheric cavity is believed to act as a resonator of MHD oscillations much as the entire magnetosphere at times oscillates in an MHD cavity-mode oscillation (ALLAN *et al.*, 1986; ZHU and KIVELSON, 1989).

Previous theoretical and numerical studies of the magnetospheric cavity-mode MHD oscillations treated the boundary of a cavity as a perfect reflector of wave energy (*i.e.*, LEE and LYSAK, 1989). However, FUJITA and PATEL (1992) qualitatively indicated that energy flow across the outermost L-shell of the cavity can significantly affect the behavior of cavity-mode MHD oscillations. They suggested that temporal damping of the magnetospheric cavity-mode oscillation due to the outflow across the magnetopause may be more effective than that due to ionospheric Joule dissipation.

Now we attempt to study the effect of the energy outflow numerically. Existence of the outflow means that energy of MHD oscillations is not perfectly confined in a cavity. So we call these cavity-mode oscillations imperfect cavity-mode oscillations. We briefly present here several figures showing characteristics of the imperfect cavity-mode oscillations. We restrict ourselves to discuss only the plasmaspheric cavity-mode oscillations.

2. Brief Explanation of the Model and Calculation Method

The ambient magnetic field is a dipole one. Variation of the Alfvén speed (V_A) in the meridional plane is essentially the same as that of FUJITA and PATEL (1992)

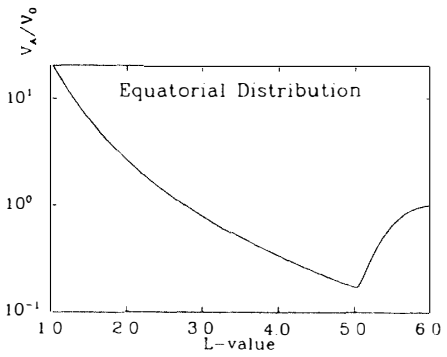

Fig. 1. Equatorial variation of V_A. The outermost L-shell is assumed at L=6. This model corresponds to the plasmasphere. The inner and outer edges of the plasmapause are located at L=5 and 6, respectively. V_A is normalized to the Alfvén speed V_0 at the equator on the outer boundary (L=6).

except that the present model has the plasmapause structure. Namely, the field-aligned variation of V_A is the same as that employed by FUJITA and PATEL (1992) (see Fig. 1-a of FUJITA and PATEL (1992)). The equatorial variation of V_A is shown in Fig. 1 where we have normalized V_A to V_0, the equatorial Alfvén speed on the outermost L-shell. As obviously shown in Fig. 1, this model has the plasmapause structure. L-values of the outermost L-shell and inner boundary of the plasmapause are 6 and 5, respectively. The entire variation of V_A in a meridional plane is given as the product of the field-aligned and equatorial variations of V_A. The outer boundary of the plasmapause corresponds to the outermost L-shell in this model.

The basic equation based on a variational formulation is given from eq. (6) of FUJITA and PATEL (1992) including Poynting flux across the boundary surface of a cavity,

$$\int_V \left\{ \frac{\omega^2 \left| \delta\vec{E}_\perp \times \hat{e} \right|^2}{V_A^2(s, L)} - \left| \nabla \times \delta\vec{E}_\perp \right|^2 \right\} dV + \int_S \hat{n} \cdot \{ \delta\vec{E}_\perp \times (\nabla \times \delta\vec{E}_\perp) \} dS = 0, \quad (1)$$

where V and S denote integration over the entire cavity (the plasmasphere in the present case) and its boundary surface, respectively. The unit vector $\hat{n}$ is directly outward and perpendicular to a magnetic L-shell. We note here that the angular frequency ω of temporal variation exp $(-i\omega t)$ becomes a complex number in our calculation. The first term corresponds to electric and magnetic field energy associated with the oscillation. Because the ionosphere is assumed to act as a perfect conductor, the last term contains only Poynting flux across the outermost L-shell.

Introducing the parameter α to describe the wave energy outflow by $\delta B_\mu = \alpha \delta E_\varphi$ on the outermost L-shell (δB_μ: field-aligned component of the magnetic field perturbation; δE_φ: azimuthal component of the electric field perturbation), the Poynting flux term of eq. (1) becomes,

$$\int_S \hat{n} \cdot \{ \delta\vec{E}_\perp \times (\nabla \times \delta\vec{E}_\perp) \} \, dS = i\omega\alpha \int_S \left| \delta E_\varphi \right|^2 dS, \quad (2)$$

assuming that α is constant over space and time, and positive α denoting outward Poynting flux across the outermost L-shell.

3. Selected Summary of the Numerical Results

We introduce two of the important results obtained by the present study. We already finished several calculations with various parameters of the model magnetosphere (including the plasmaspheric structure) and wave structure. A full description of the numerical results and implications for observations will appear in elsewhere.

3.1. Electromagnetic field perturbations of the imperfect cavity-mode oscillation

Figure 2 shows the spatial structure of the electromagnetic (EM) field perturbation associated with the imperfect cavity-mode oscillation with zero m (the azimuthal wave number) in the northern hemisphere. In this calculation α is 1. This mode is the pure fast magnetosonic (compressional, poloidal) wave with the normalized

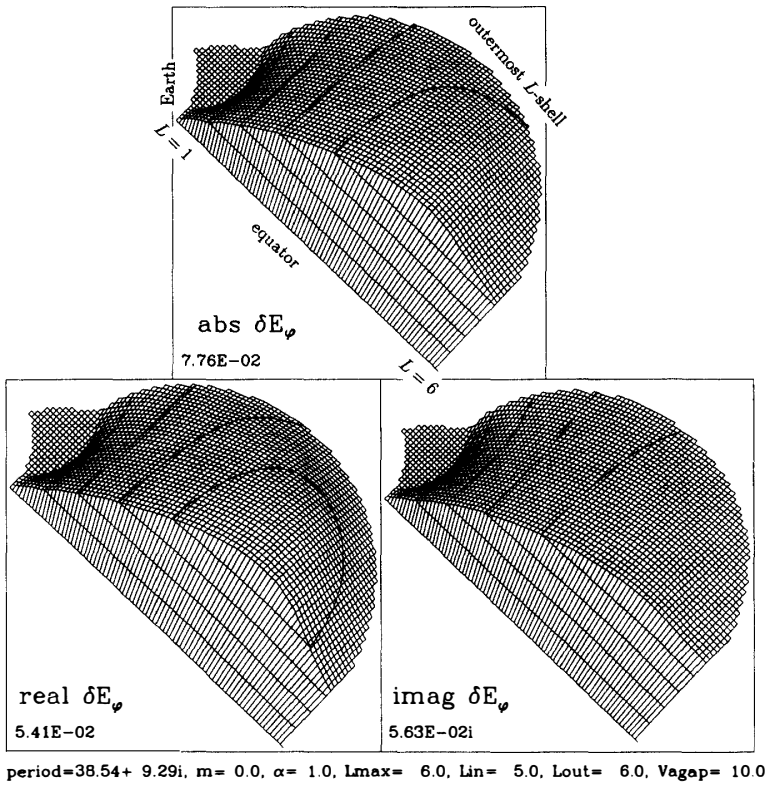

Fig. 2a

Fig. 2. Birds-eye-views of spatial structures of EM field perturbation associated with the imperfect cavity-mode oscillation for the case of α = 1 and m = 0 in the northern hemisphere. The straight line from upper-left (the Earth side) to lower-right (the outermost L-shell; the plasmapause in this figure) means the equator.
The eigenperiod (normalized to R_e/V_0) is 38.54+9.29i ($\omega R_e/V_0$ = 0.154–0.037i). (a) δE_φ (b) δB_r, (c) δB_μ. The numeral shown in the lower-left corner of each figure is the amplitude directly obtained from the FEM calculation.

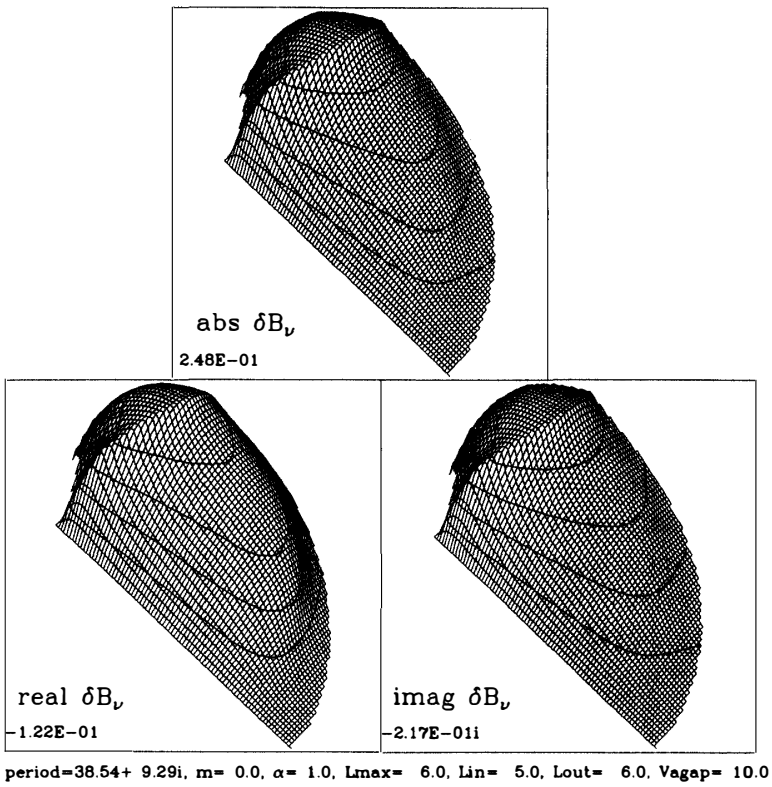
abs δB_ν
2.48E-01
real δB_ν
-1.22E-01
imag δB_ν
-2.17E-01i
period=38.54+ 9.29i, m= 0.0, α= 1.0, Lmax= 6.0, Lin= 5.0, Lout= 6.0, Vagap= 10.0

Fig. 2b.

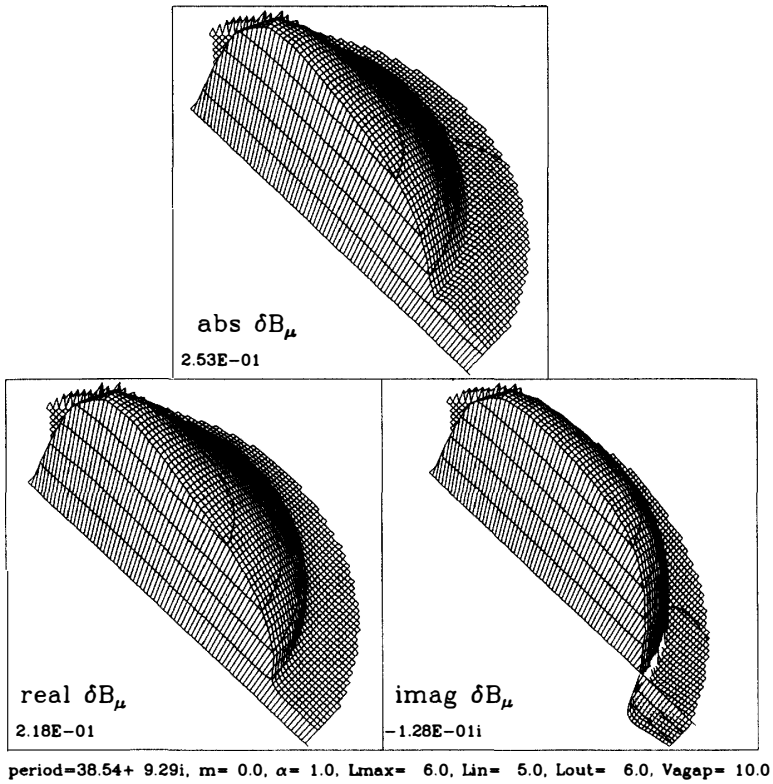
abs δB_μ
2.53E-01
real δB_μ
2.18E-01
imag δB_μ
-1.28E-01i
period=38.54+ 9.29i, m= 0.0, α= 1.0, Lmax= 6.0, Lin= 5.0, Lout= 6.0, Vagap= 10.0

Fig. 2c.

eigenperiod of $38.54+9.29i$ ($\omega R_e/V_0 = 0.154-0.037i$ where R_e is Earth's radius). Therefore this has δE_φ, δB_ν (radial component of magnetic field perturbation), and δB_μ. This figure presents birds-eye-views of real, imaginary parts and intensity of each EM field perturbation. Because these figures seem to be unfamiliar to readers, let us explain how to recognize the perturbation amplitude from them. Let x and y be $x = r\sin\theta$ and $y = r\cos\theta$ where r and θ are the geocentric distance and the colatitude from the north pole. Then the real part of δE_φ, for example, forms a curved surface on the plane (x,y) when (x,y) lies in a horizontal plane and the real part of δE_φ is plotted on the z-axis. The birds-eye-view method is employed to show this surface. When t is zero we have the electric field perturbation shown in *real* of Fig. 2. When t becomes π/real (2ω) it becomes that in *imag* of Fig. 2. The eye point is common to all figures and the each field perturbation is normalized to its maximum value. This is the fundamental mode of the imperfect cavity-mode oscillation.

The damping is attributed to energy escape across the plasmapause. It is characteristic that the damping rate ($\gamma = 0.037$) to angular frequency (real $\omega = 0.154$) ratio (γ/real ω) is very large (~0.25). This means that this mode is not trapped sufficiently in the cavity. Indeed, electric field structure presented in Fig. 2a shows comparatively large amplitude on the outermost L-shell (plasmapause). The perfectly reflected outermost L-shell boundary assumed by previous works yields zero δE_φ there.

The spatial structure of the EM field perturbation shown in Fig. 2 is similar to that analyzed from satellite data by TAKAHASHI *et al.* (1992) who suggested that the magnetic fields of the ULF oscillation do not have a node nor a bulk on the plasmapause. But they regarded the plasmaspheric MHD oscillation as a wave generated by some external pumping wave. This situation is reproduced by a negative value of α in our calculation. When α is -1 instead of 1 (the value used for Fig. 2), the spatial structure of the EM field perturbation remains the same except that the phase relation between δE_φ and δB_μ becomes reversed. This feature, indicating that the direction of the radial Poynting flux is reversed, gives positive γ in the case of negative α.

3.2. Damping of the coupled mode oscillation

When m becomes nonzero, the fast magnetosonic wave and the Alfvén wave are coupled.

The damping rate is larger when the coupled cavity-mode oscillation is originally derived from the fast magnetosonic wave (when m is zero, the mode is reduced to the pure fast magnetosonic wave.) The damping is smaller for the coupled mode oscillation originating from the Alfvén wave. The pure Alfvén wave does not have radial Poynting flux which transports wave energy outside of the cavity. Therefore it is originally not a damped oscillation even when the cavity is imperfect. But the fast magnetosonic wave generated through the coupling transports the flux and contributes to the damping. Therefore damping is a secondary effect due to the coupling. In addition to the pure fast magnetosonic wave, there is a damped oscillation in the imperfect cavity as investigated above. As a result we can understand the difference in the damping rate stated above.

3.3. *Remarks*

We should note here that the oscillation obtained by the present numerical calculation is the eigenmode one in the cavity. Therefore when we apply the results to transient phenomena such as Pi2 pulsations, we should be careful that temporal damping of the oscillations is attributed to two possible mechanisms; the first is the energy escape from the cavity described in the presented paper and the other is transient behavior of a source wave. We need to employ a transient model to distinguish the two damping mechanisms. Bearing in mind that the plasmasphere is an imperfect cavity for MHD oscillations, we can conclude that the mechanism stated in the present paper will work to some extent.

Acknowledgments

The authors are grateful to Dr. K. TAKAHASHI of the Solar-Terrestrial Environment Laboratory, Nagoya University for valuable discussions. They are also grateful to Dr. YEOMAN of Leicester University for sending us reference papers. One of the authors (S.F.) thanks Dr. V. L. PATEL of Naval Research Laboratory for introducing him to the Finite Element Method calculation. Numerical calculations have been done at the Computer Center of the Meteorological Research Institute and the National Institute of Polar Research.

References

ALLAN, W., POULTER, E. M. and WHITE, S. P. (1986): Hydromagnetic wave coupling in the magnetosphere-plasmapause effects on impulse-excited resonances. Planet. Space Sci., **34**, 1189–1200.

FUJITA, S. and PATEL, V. L. (1992): Eigenmode analysis of coupled magnetohydrodynamic oscillations in the magnetosphere. J. Geophys. Res., **97**, 13777–13788.

LEE, D.-H. and LYSAK, R. (1989): Magnetospheric ULF wave coupling in the dipole model: The impulsive excitation. J. Geophys. Res., **94**, 17097–17103.

SUTCLIFFE, P. R. and YUMOTO, K. (1989): Dayside Pi2 pulsations at low latitudes. Geophys. Res. Lett., **16**, 887–890.

SUTCLIFFE, P. R. and YUMOTO, K. (1991): On the cavity mode nature of low-latitude Pi2 pulsations. J. Geophys. Res., **94**, 1543–1551.

TAKAHASHI, K., OHTANI, S.-I. and YUMOTO, K. (1992): AMPTE CCE observations of Pi 2 pulsations in the inner magnetosphere. Geophys. Res. Lett., **19**, 1447–1450.

YEOMAN, T. K. and ORR, D. (1989): Phase and spectral power of mid-latitude Pi2 pulsations: Evidence for a plasmaspheric cavity resonance. Planet. Space Sci., **37**, 1367–1383.

YUMOTO, K., TAKAHASHI, K., SATO, T., MENK, F. W., FRASER, B. J., POTEMRA, T. A. and ZANETTI, L. J. (1989): Some aspects of the relation between Pi 1–2 magnetic pulsations observed at L=1.3–2.1 on the ground and substorm-associated magnetic field variations in the near-Earth magnetotail observed by AMPTE CCE. J. Geophys. Res., **94**, 3611–3618.

ZHU, Z. and KIVELSON, M. G. (1989): Global mode ULF pulsations in a magnetosphere with a non-monotonic Alfvén velocity profile. J. Geophys. Res., **94**, 1479–1485.

(Received April 2, 1993; Revised manuscript received April 19, 1993)